Supplementary Information

HACS1 signaling adaptor protein recognizes a motif in the Paired Immunoglobulin Receptor B cytoplasmic domain

Jamie J Kwan, Sladjana Slavkovic, Michael Piazza, Dingyan Wang, Thorsten Dieckmann, Philip E. Johnson, Xiao-Yan Wen, and Logan W Donaldson

Category	Available	Assigned	% assigned
Element C	300	257	85.7
Element H	367	341	92.9
Element N	79	61	77.2
Backbone + H + HA	307	295	96.1
Backbone	183	173	94.5
Side chain H	243	219	90.1
Side chain non-H	196	145	74.0

Table S1 — Chemical shift assignment summary for the HACS1 SH3 domain (aa. 27-87). The first twenty-six amino acids are unassigned. This table was produced by CCPN Analysis v2.4.

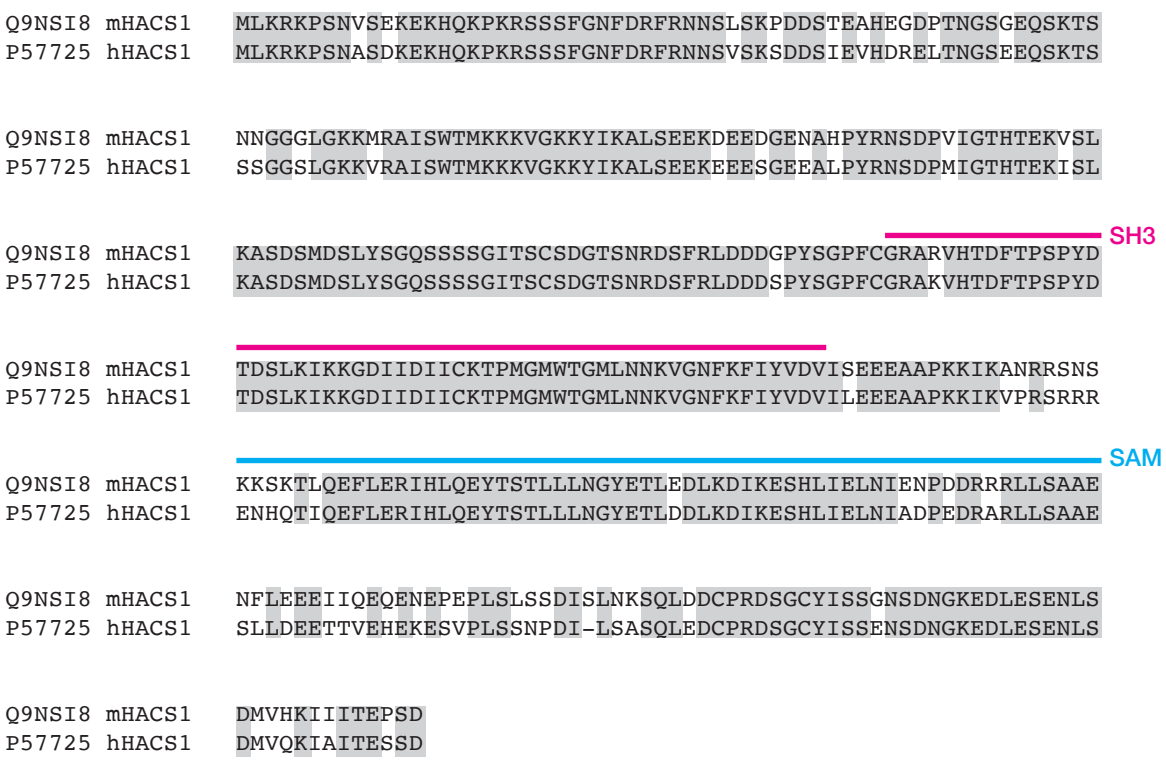

Figure S1 — Sequence alignment of murine and human HACS1. Each protein is also referenced by its Uniprot code. Shading indicates identity. The SH3 and SAM domains are indicated.

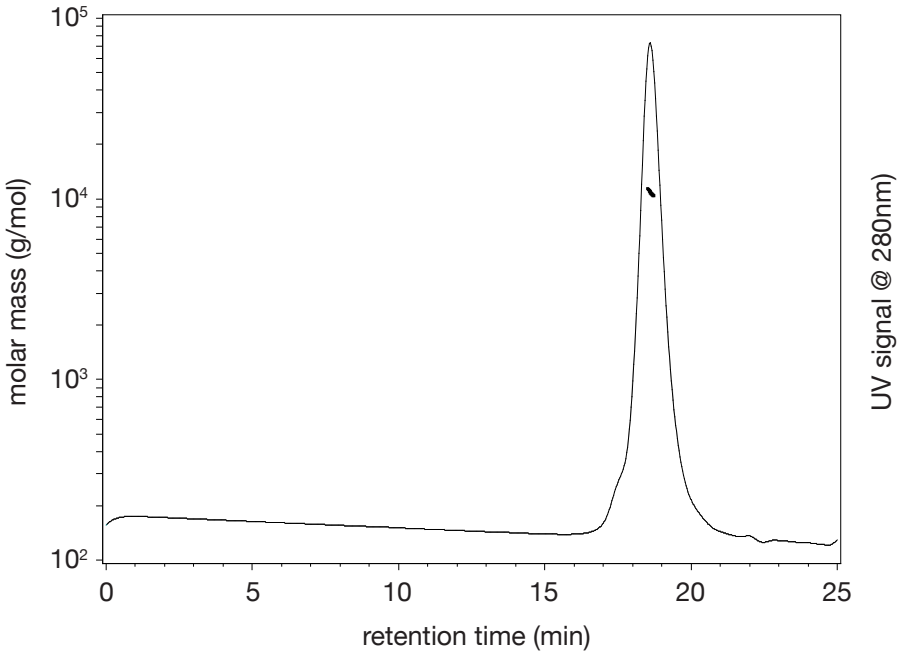

Figure S2 — Size exclusion chromatography with multi-angle laser scatter (SEC-MALS) analysis. 20 uL of 2 mg/mL HACS1 SH3 domain was subjected to chromatography (mobile phase: phosphate buffered saline) and detection by UV absorbance, MiniDAWN TREOS MALS, and OptiLAB T-rEX refractive index instruments. After data processing, the the observed peak coincides with a molecular mass of 10.9 ± 0.3 kDa suggesting that the HACS1 SH3 domain is monomeric (expected molecular mass, 10.65 kDa).

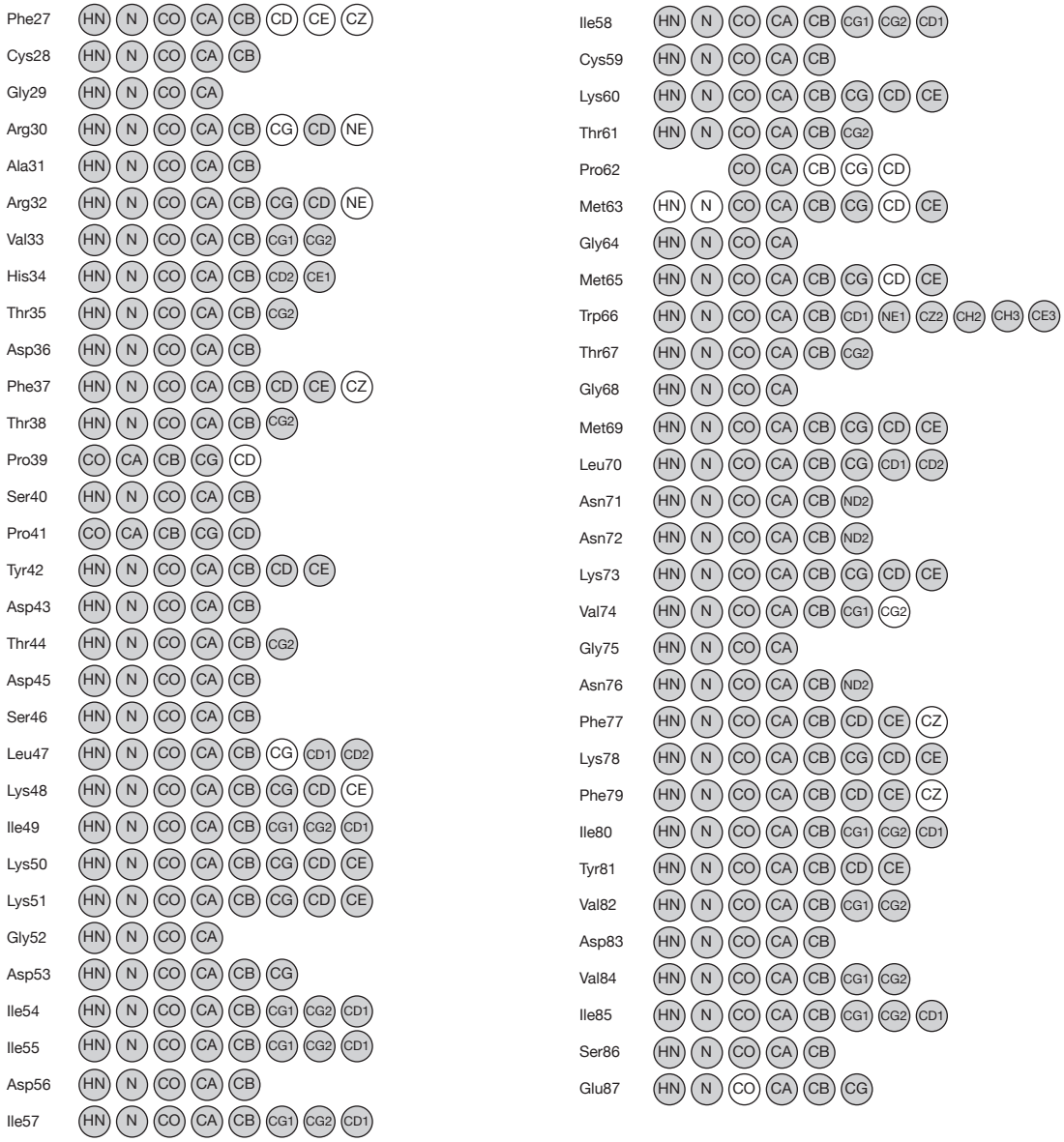

Figure S3 — Graphical summary of backbone and side chain heavy atom assignments for the HACS1 SH3 domain. The first twenty-six amino acids of the protein fragment are unassigned. Shading indicates that an assignment was made.

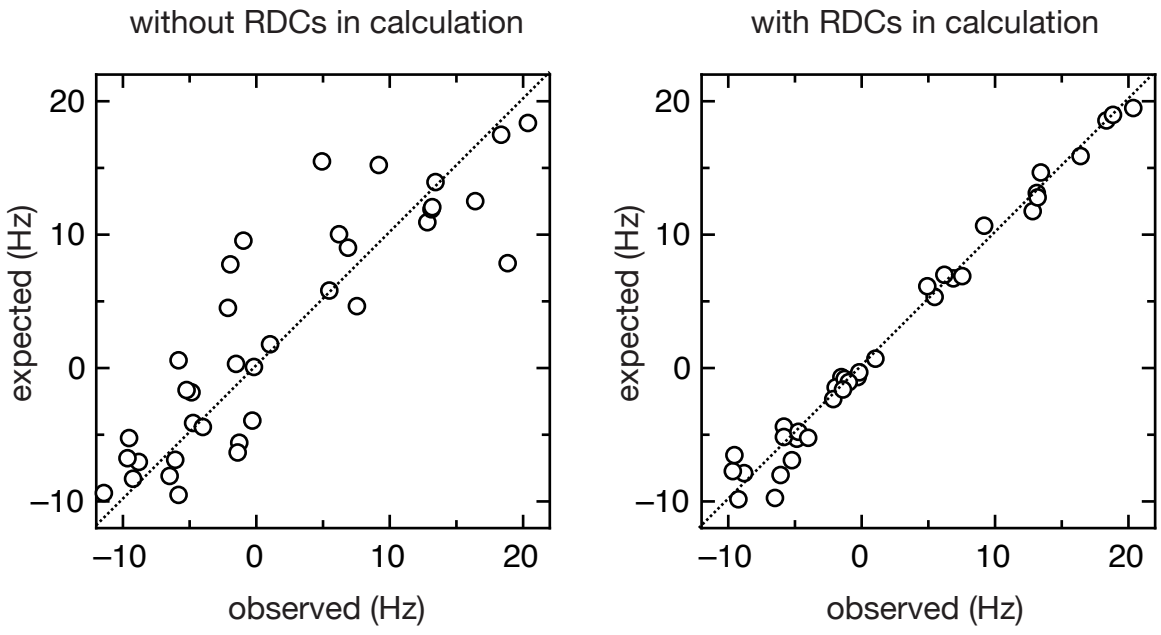

Figure S4 — Scatter plot of observed and expected HN residual dipolar couplings (RDCs) for the lowest energy structure of an ensemble that was calculated without or without the RDC dataset (n=42). Statistics are presented in Table 1 of the main text.

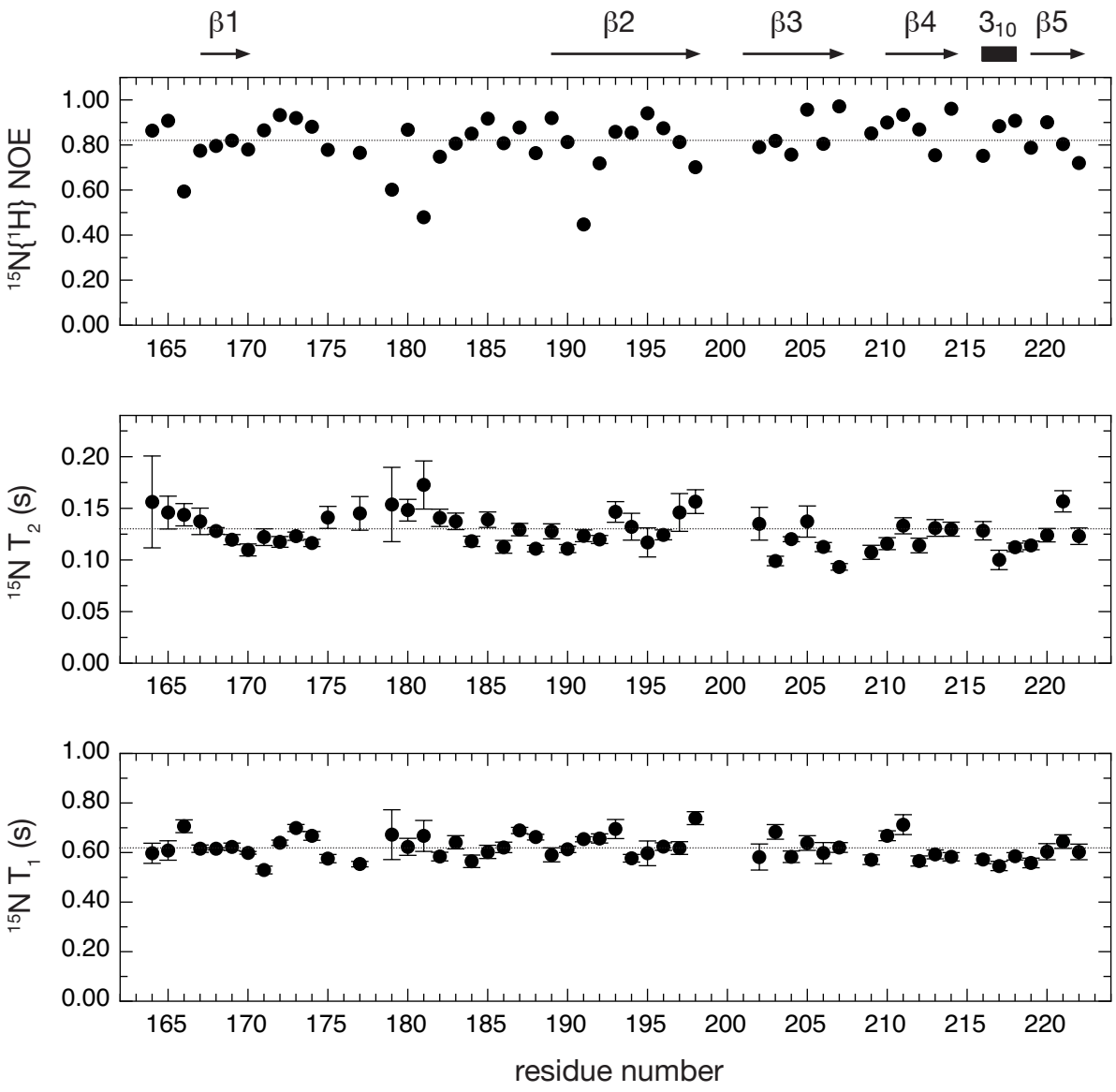

Figure S5 — NMR relaxation analysis of the HACS1 SH3 domain. Data were acquired at 25°C on a 700 MHz spectrometer. Observed secondary structures are indicated above the graphs for reference. A dotted line indicates the average value. Error bars indicate the standard deviation of the fit to a monoexponential rate.

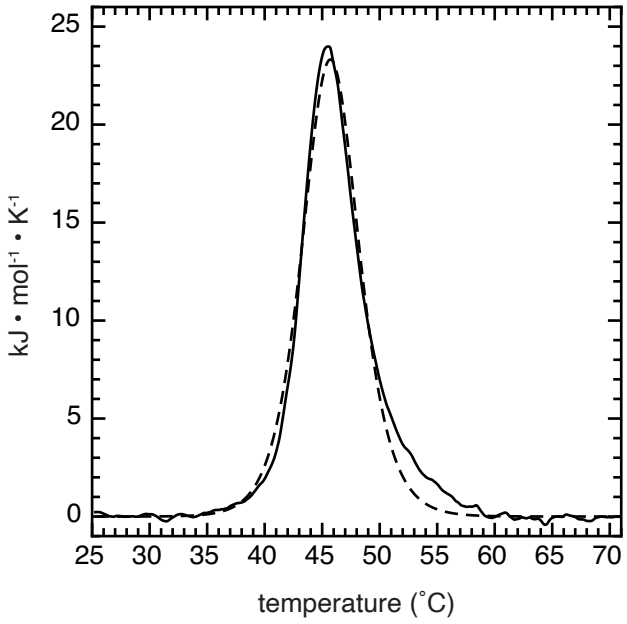

Figure S6 — Differential scanning calorimetry of the HACS1 SH3 domain. The unfolding was not reversible with a thermal transition midpoint (T_m) of 47.5 ˚C.

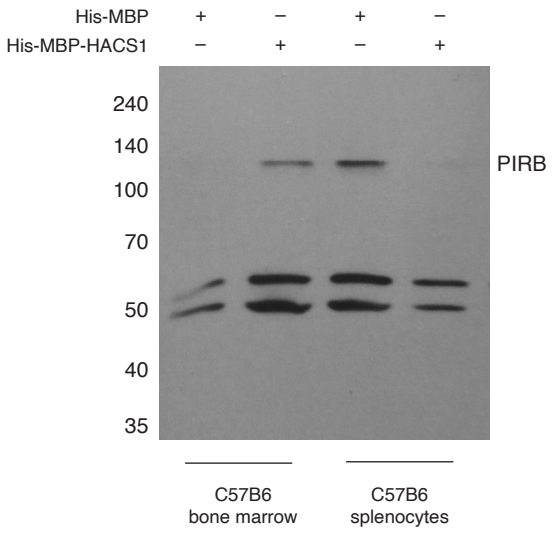

Figure S7 — Western detection of the HACS1-PIRB interaction. Immunoprecipitations: Lanes 1 and 2: C57B6 mouse bone marrow protein lysate with 6xHis-MBP control protein and 6xHis-MBP-HACS1-SH3 protein, respectively. Lanes 3 and 4: C57B6 mouse splenocyte protein extract with 6xHis-MBP-HACS1-SH3 protein and 6xHis-MBP control protein, respectively.

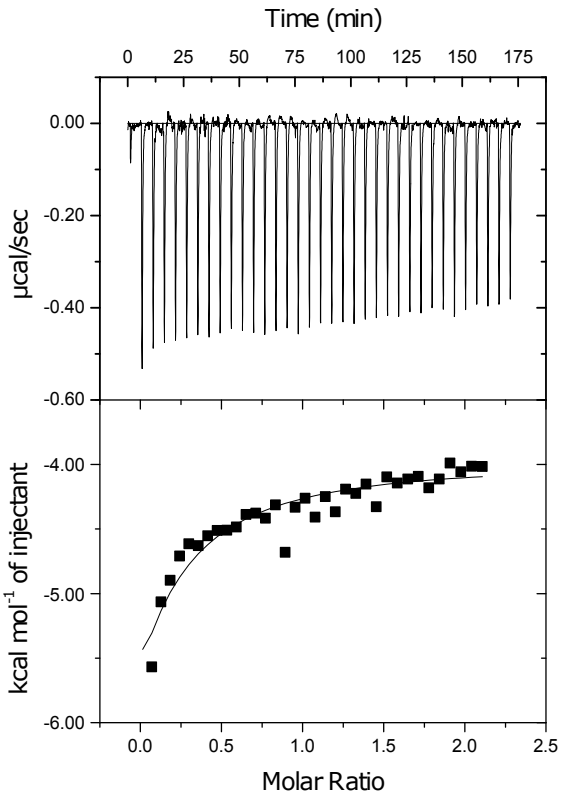

Figure S8 — Isothermal titration calorimetry. A reaction cell containing 91 uM HACS1 SH3 domain in 20 mM Tris pH 7.9, 50 mM NaCl, 1 mM TCEP was titrated with a 1.0 mM murine PIRB ITIM3 sequence fused amino-terminally to the Protein G B1 domain for enhanced solubility. This figure represents data that were adjusted for heat of dilution. The data were fit to 1:1 binding equilibrium with K_D of 15.9 uM.

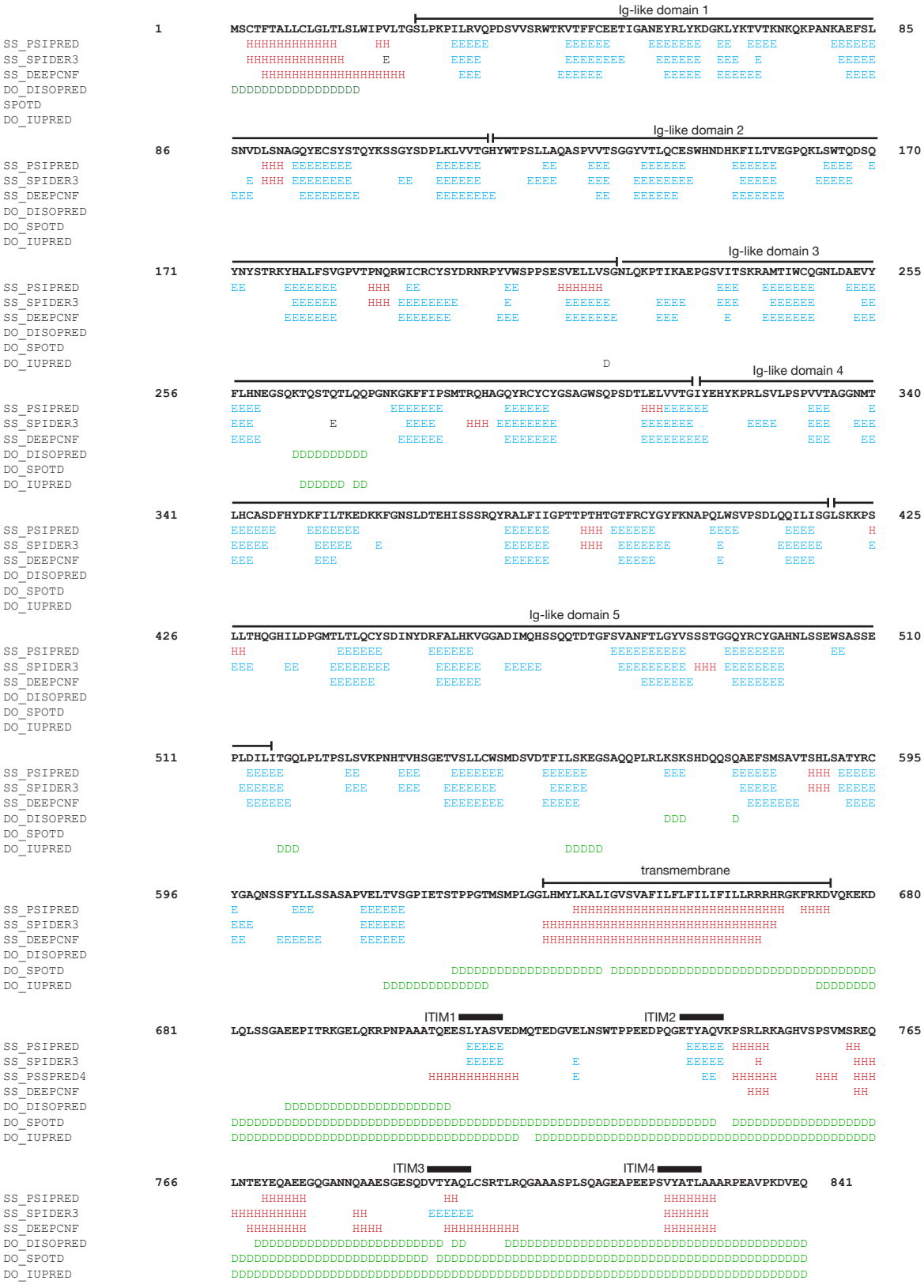

Figure S9 — Sequence analysis of murine PIRB. Helical (H), strand (S) and disordered (D) regions were predicted by PSIPRED (Buchan & Jones. 2019. Nucl Acids Res 47: W402), SPIDER3 (Heffernan *et al*. 2017. Bioinformatics 33:2842), DEEPCNF (Wang *et al.* 2016. Sci Rep 11:18962), DISOPRED3 (Jones & Cozzetto. 2015. Bioinformatics 31: 857), SPOTD (Hanson *et al.* 2017. Bioinformatics 33: 685) and IUPRED (Dosztányi *et al.* 2005. J Mol Biol 347: 827). The Ig repeats, transmembrane region, and ITIMs 1-4 are indicated. Ig-like domain boundaries are derived from the PIRB extracellular domain crystal structure (PDB:6GRQ; Vlieg et al. 2019. J Biol Chem 294: 4634).